Analysis and Control of Quadcopter System

Dina Mohamed Saad †‡, Marwa Lotfy Ismail †‡, Nada Tamer Abdelhay †‡, Kareem Hindi †‡, Ahmed Abdulhameed †‡,
* Cairo, Egypt
† Mechatronics Department - Faculty of Engineering and Materials Science - German University in Cairo, Egypt
Emails: dina67724@gmail.com, lotfymarwa410@gmail.com, nadatameer@outlook.com, kareem.hindi12@gmail.com, Ahmed.elessawy@student.guc.edu.eg

***Abstract*—Quadcopters are widely used in different applications. Modeling and control of the quadcopter are challenging due to its highly nonlinear dynamics. This paper covers the analysis and the stability of the nonlinear system of quadcopters using Lyapunov stability criteria. In addition to that, the controller is designed to track the desired position and orientation. The proposed control method is tested on both simulation and hardware and results are analyzed using MATLAB/Simulink.**

***Index Terms*—Quadcopters, Quadrotors, Lyapunov stability, nonliner, control**

Fig. 1: Quadcopter Applications

I. Introduction

Quadcopters, also known as quadrotors are one of the examples for aerial vehicles , which operate with four rotors. Moreover, they are used in a wide area of applications like aerial photography and surveillance, making them useful in the area of search, rescue and environmental monitoring. In addition, they can be used in delivery services for small packages, especially in remote and congested areas.

In order to discuss the study outcomes, the remainder of the paper is organized as follows: section II presents the dynamic model and Lyapunov stability analysis. The controller design is discussed through section III, section IV includes the results of the conducted simulations. Hardware implementation and results are illustrated through section V. Finally, section VI summarizes the conducted work and recommends future endeavors of this study.

II. Modeling

The quadcopter dynamics are modeled in by the governing equations:

$$\begin{aligned}
\ddot{x} &= (\cos\phi \sin\theta \cos\psi + \sin\phi \sin\psi) \cdot u_1/m \\
\ddot{y} &= (\cos\phi \sin\theta \sin\psi - \sin\phi \cos\psi) \cdot u_1/m \\
\ddot{z} &= -g + (\cos\phi \cos\theta) \cdot u_1/m \\
\ddot{\phi} &= \dot{\theta}\dot{\psi}\left(\frac{I_y - I_z}{I_x}\right) - \frac{J_R}{I_x}\dot{\theta}\omega_d + \frac{l}{I_x}u_2 \\
\ddot{\theta} &= \dot{\phi}\dot{\psi}\left(\frac{I_z - I_x}{I_y}\right) + \frac{J_R}{I_y}\dot{\phi}\omega_d + \frac{l}{I_y}u_3 \\
\ddot{\psi} &= \dot{\phi}\dot{\theta}\left(\frac{I_x - I_y}{I_z}\right) + \frac{l}{I_z}u_4
\end{aligned}$$

such that the input for the system are:

$$\begin{aligned}
u_1 &= b\left(\omega_1^2 + \omega_2^2 + \omega_3^2 + \omega_4^2\right) \\
u_2 &= b\left(\omega_4^2 - \omega_2^2\right) \\
u_3 &= b\left(\omega_3^2 - \omega_1^2\right) \\
u_4 &= d\left(\omega_2^2 + \omega_4^2 - \omega_1^2 - \omega_3^2\right)
\end{aligned}$$

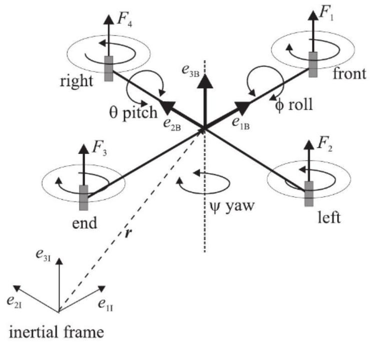

Fig. 2: Frames and configuration

and the definition of a new variable:

$$\omega_d = \omega_2 + \omega_4 - \omega_1 - \omega_3$$

For the state space representations of the system:

$$= \begin{pmatrix} x_2 \\ (\cos x_7 \sin x_9 \cos x_{11} + \sin x_7 \sin x_{11}) \cdot u_1/m \\ x_4 \\ (\cos x_7 \sin x_9 \sin x_{11} - \sin x_7 \cos x_{11}) \cdot u_1/m \\ x_6 \\ -g + (\cos x_7 \cos x_9) \cdot u_1/m \\ x_8 \\ x_{12} x_{10} I_1 - \frac{J_R}{I_x} x_{10} \omega_d + \frac{l}{I_x} u_2 \\ x_{10} \\ x_{12} x_8 I_2 + \frac{J_R}{I_y} x_8 \omega_d + \frac{l}{I_y} u_3 \\ x_{12} \\ x_{10} x_8 I_3 + \frac{l}{I_z} u_4 \end{pmatrix}$$

III. Control Design

IV. Simulation and results

A. Open Loop Response

The Quadcopter open loop response was simulated under n case studies, where different combinations of input motor rps (rad per seconds) (w1,w2,w3,w4) are tested to plot the response of the drone states, namely the position and orientation:(x,y,z,phi,theta,psi) and the velocity (x,y,z,phi,theta,psi) dot.

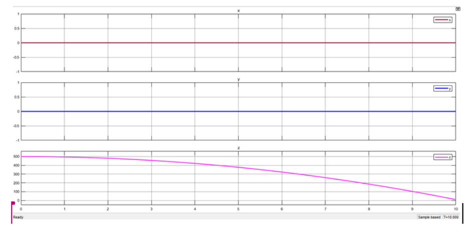
Fig. 3: Case 1:Linear Positions

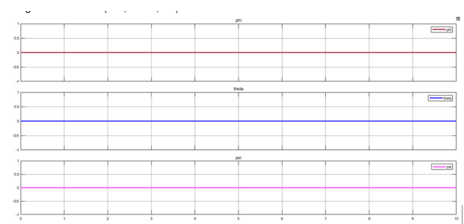
Fig. 4: Case 1:Angular positions

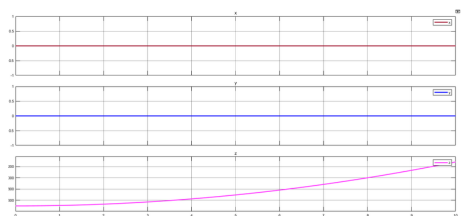
Fig. 5: Case 2:Linear Positions


Fig. 6: Case 2:Angular positions

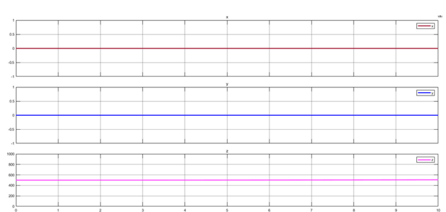
Fig. 7: Case 3:Linear Positions

TABLE I: DH Parameters Table

Case Study	w_1	w_2	w_3	w_4
Case 1	0	0	0	0
Case 2	1000	1000	1000	1000
Case 3	625	625	625	625
Case 4	0	625	0	625

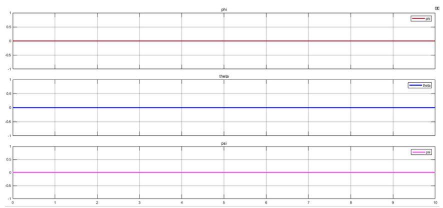

Fig. 8: Case 3:Angular positions

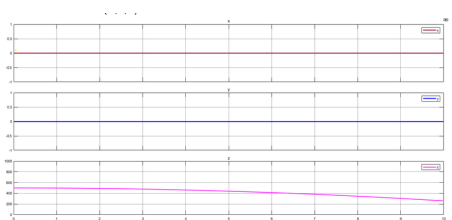

Fig. 9: Case 4:Linear Positions

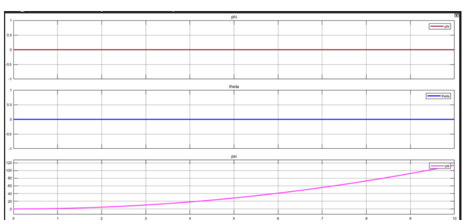

Fig. 10: Case 4:Angular positions

V. Closed loop control

The control strategy has been executed to regulate the altitude and position of the quadcopter through the utilization of the vertical thrust input U_1. The position controller provides the desired roll and pitch angles based on the quadcopter's altitude and position, which are then fed to the attitude controller. The attitude and heading controllers work to stabilize the quadcopter under quasi-stationary conditions, employing control inputs U_2, U_3, and U_4 respectively.

A. Sliding Mode Control

This section aims to provide a thorough elucidation of the development of a control law based on Sliding Mode Control (SMC) to regulate the quadcopter's attitude, heading, altitude, and x, y position. Building upon the work conducted by Tripathi et al. in [1], this approach ensures a comprehensive understanding of the dynamics and parameters involved in achieving precise control over the quadcopter's multiple degrees of freedom.

$$\left.\begin{aligned} a_1 &= \tfrac{J_y - J_z}{J_x}, b_1 = \tfrac{l}{J_x} \\ a_2 &= \tfrac{J_z - J_x}{J_y}, b_2 = \tfrac{l}{J_y} \\ a_3 &= \tfrac{J_x - J_y}{J_z}, b_3 = \tfrac{1}{J_z} \end{aligned}\right\}$$

1) Roll control: Let the tracking error in roll angle is defined as:

$$e_1 = \phi - \phi_d$$

The sliding surface for roll control is defined as,

$$s = \dot{e_1} + c_1 e_1$$

Derivative of sliding surface will therefore be:

$$\dot{s} = c_1 \left(\dot{\phi} - \dot{\phi}_d\right) + \ddot{\phi} - \ddot{\phi}_d$$

To satisfy the sliding mode condition $s\dot{s} < 0$, the value of k_1 and k_2 is chosen such that $k_1 > 0$ and $k_2 > 0$.

By equating the proposed reaching law Eq.(18) to the derivative of the sliding surface in Eq.(16) and substituting $\ddot{\phi}$ from Eq.(9), the control input U_2 can be extracted as:

$$U_2 = \frac{1}{b_1}\left[-k_1 \operatorname{sgn}(s) + k_2 s - a_1 \dot{\theta}\dot{\psi} + \ddot{\phi}_d + c_1\left(\dot{\phi}_d - \dot{\phi}\right) + \frac{J_R}{I_x}\dot{\theta}\omega_d\right]$$

$$U_3 = \frac{1}{b_2}\left[-k_3 \operatorname{sgn}(s) + k_4 s - a_2 \dot{\phi}\dot{\psi} + \ddot{\theta}_d + c_2\left(\dot{\theta}_d - \dot{\theta}\right) - \frac{J_R}{I_x}\dot{\theta}\omega_d\right]$$

3) Yaw or heading control: Similarly the control input U_4 responsible for generating the yaw rotation ψ can be calculated as:

$$U_4 = \frac{1}{b_3}\left[-k_5 \operatorname{sgn}(s) + k_6 s - a_3 \dot{\phi}\dot{\theta} + \ddot{\psi}_d + c_3\left(\dot{\psi}_d - \dot{\psi}\right)\right]$$

4) Atitude control: Similarly the control input U_1 responsible for generating the vertical motion z can be calculated as:

$$U_1 = \frac{m}{\cos\phi\cos\theta}\left[-k_7 \operatorname{sgn}(s) + k_8 s + g + \ddot{z}_d + c_4\left(\dot{z}_d - \dot{z}\right)\right]$$

5) x and y Motion Control: Consider U_x and U_y are the orientations of U_1 which is responsible for the x and y motion respectively, can be extracted in a similar way as:

$$U_x = \frac{m}{U_1}\left[k_9 \operatorname{sgn}(s) + k_{10} s + \ddot{x}_d + c_5\left(\dot{x}_d - \dot{x}\right)\right]$$
$$U_y = \frac{m}{U_1}\left[k_{11} \operatorname{sgn}(s) + k_{12} s + \ddot{y}_d + c_6\left(\dot{y}_d - \dot{y}\right)\right]$$

VI. State flow diagram

The state flow chart illustrates the dynamic behavior and control logic of the quadcopter system utilizing Sliding Mode Control (SMC). The various states represent distinct operational modes, each characterized by specific behaviors and control strategies. The transitions between states are governed by predefined conditions, encapsulating the system's response to external stimuli, commands, and inherent sensor feedback.

The flow chart provides a visual representation of the quadcopter's operational states and the decision-making process governing state transitions. It serves as a valuable tool for understanding the system's behavior and the application of Sliding Mode Control in various scenarios.

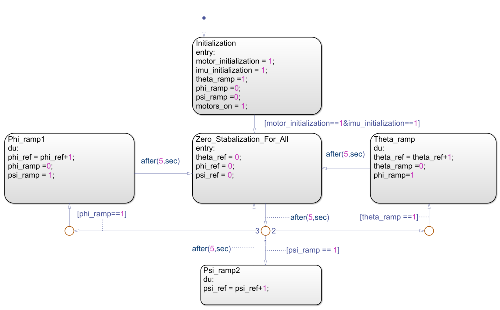

Fig. 11: Complete state flow chart of the Quadcopter.

VII. Hardware Implementation

The quadcopter is fixed on a spherical joint on a pole since we only need to stabilize it, and the quadcopter is not ready to take off yet, the controller is supplied using an Arduino Uno R3, which takes commands from a mounted Raspberry Pi 4 that communicates with, ensuring that if something happens the Arduino will take the damage and protect the raspberry pi.

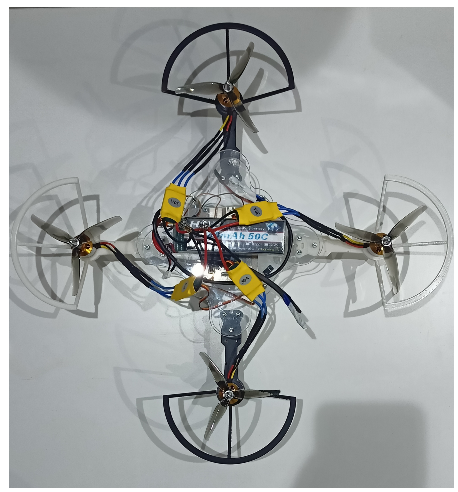

Fig. 12: Fabricated Quadcopter

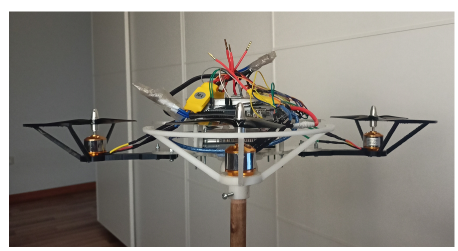

Fig. 13: Mounted Quadcopter

VIII. Results of Sliding Mode Control for Quadcopter

The drone was constructed utilizing two distinct machines. Initially, a 3D printer was employed to fabricate the motor arms using PLA as the chosen material. Subsequently, a CNC laser cutting machine was utilized to cut two acrylic sheets, forming both the base and the top plate of the drone. Additionally, a coupling was 3D printed with PLA to securely affix the drone to the ground

A. *Sliding Mode Control Simulation Results*

The application of Sliding Mode Control (SMC) to the quadcopter has yielded promising results, demonstrating its effectiveness in achieving precise control over the desired orientation and position. The controller was designed to handle both constant values and ramp inputs for orientation and position tracking.

B. *Orientation Control*

In the case of orientation control, the quadcopter exhibited robust performance in maintaining the desired roll, pitch, and yaw angles. The sliding mode controller effectively countered external disturbances and uncertainties, ensuring that the quadcopter adhered closely to the specified orientation trajectory. This was evident in both constant values and ramp inputs, showcasing the versatility of the control strategy.

C. *Position Control*

Similarly, the sliding mode control strategy demonstrated remarkable capabilities in positioning the quadcopter accurately in the desired x and y coordinates. Whether tasked with holding constant positions or tracking ramp inputs, the quadcopter showcased stability and responsiveness in its movements. The sliding mode controller facilitated precise trajectory tracking, even in the presence of disturbances.

D. *Overall Performance*

The overall performance of the sliding mode control for the quadcopter was characterized by its ability to provide robust and adaptive control. The system showcased resilience to uncertainties and disturbances, ensuring that the quadcopter achieved and maintained the desired orientation and position as dictated by the control inputs. The transition between constant values and ramp inputs was smooth, underscoring the controller's effectiveness in handling dynamic scenarios.

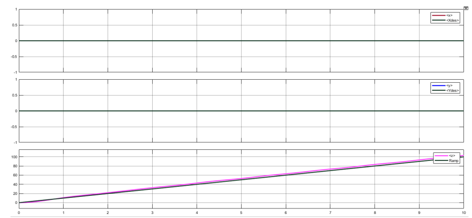

Fig. 14: Tracking step z position

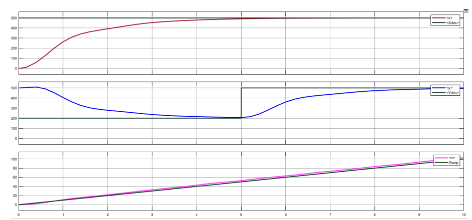

Fig. 15: Tracking xyz

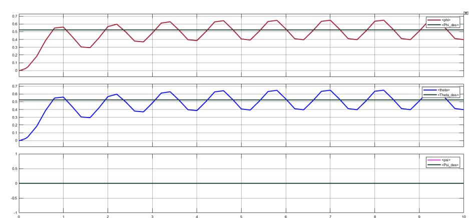

Fig. 16: Tracking step roll and pitch

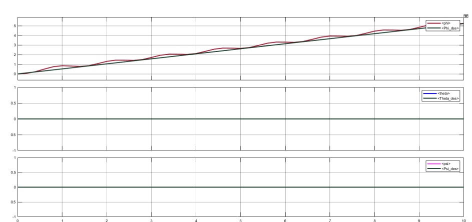

Fig. 17: Tracking ramp roll

References

References

[1] Vibhu Kumar Tripathi, Laxmidher Behera, Nishchal Verma, *Design of sliding mode and backstepping controllers for a quadcopter*, In: *2015 39th National Systems Conference (NSC)*, Year: 2015, Pages: 1-6, DOI: 10.1109/NATSYS.2015.7489097